DOI: 10.4408/IJEGE.2011-03.B-110

AN EMPIRICAL METHOD TO FORECAST THE EFFECT OF STORM INTENSITY ON SHALLOW LANDSLIDE ABUNDANCE

JONATHAN D. STOCK(*) & DINO BELLUGI(**),(***)

(*)U.S. Geological Survey, 345 Middlefield Road, Menlo Park, CA, 94025, USA; jstock@usgs.gov
(**)University of California, Department of Earth & Planetary Science, Berkeley, CA, USA
(***)University of California, Department of Computational Science and Engineering, Berkeley, CA, USA

ABSTRACT

We hypothesize that the number of shallow landslides a storm triggers in a landscape increases with rainfall intensity, duration and the number of unstable model cells for a given shallow landslide susceptibility model of that landscape. For selected areas in California, USA, we use digital maps of historic shallow landslides with adjacent rainfall records to construct a relation between rainfall intensity and the fraction of unstable model cells that actually failed in historic storms. We find that this fraction increases as a power law with the 6-hour rainfall intensity for sites in southern California. We use this relation to forecast shallow landslide abundance for a dynamic numerical simulation storm for California, representing the most extreme historic storms known to have impacted the state.

KEY WORDS: *landslide susceptibility, storm intensity, landslide frequency*

INTRODUCTION

Intense rainfalls from historic storms have triggered widespread shallow landslides in the coastal mountains of California, USA (e.g., RICE & FOGGIN, 1971; TAYLOR & BRABB, 1972; CAMPBELL, 1975; NILSEN & TURNER, 1975; TAYLOR *et alii*, 1975; NILSEN *et alii,* 1976a,b; WENTWORTH, 1986; ELLEN & WIECZOREK, 1988; GODT *et alii*, 1999; COE & GODT, 2001). These landslides may occur during or soon after the most intense rainfall (e.g., CAMPBELL, 1975, MONTGOMERY *et alii,* 2009), and involve failure of soil and weathered bedrock layers. They are commonly fractions of a meter to several meters deep, rarely exceeding ~10 m in width or length. A fraction of these failures mobilize as debris flows, mixtures of soil, water and rock that sweep down steep valleys at high velocities and destroy homes and infrastructure with little warning.

Varved sediments in the Santa Barbara basin, southern California, may contain the geologic record of the largest storms over the past millennium (SCHIMMELMAN *et alii*, 2003). Layers interpreted as storm deposits have a periodicity of several hundred years, not unlike earthquake recurrence intervals for the San Andreas Fault. These deposits are substantially thicker than those associated with storms of January 1969, the most recent historic events to generate widespread landslides in southern California. If layer thickness scales with storm intensity, these layers imply that southern California has experienced storms that are massive compared to our recent historical experience. Unlike seismic hazard maps available for some large faults, we cannot begin to quantify the magnitude of landslide hazards that will accompany such a storm. Put simply, we cannot answer the question of how many shallow landslides California's largest storms would trigger

We are beginning to understand more about what such massive storms might look like. Recent work (RALPH *et alii*, 2006; NEIMAN *et alii*, 2008) illustrates that some of California's largest storms are atmos-

pheric rivers of moisture that originate in the tropics and convey vast amounts of water vapor towards California in a narrow jet (e.g., 100-200 km wide) of moisture. Where these jets strike California, they can deliver record rainfalls and river discharges over the course of 1-3 days. Consequently, depending on their intensity and occupation time, they can cause widespread landsliding (e.g., Southern California storm of January 1969). The storms of 1861/62, largest in California's recorded history, may represent the most recent great atmospheric river to hit California, and may be an example of the kind of storms that are recorded in the Santa Barbara basin deposits.

As part of an exercise to simulate the hazards from a great storm, Dettinger *et alii* (2011) simulated an atmospheric river storm (Arkstorm) using 1969 and 1985 atmospheric data as initial and boundary conditions in a dynamic meteorological model. They used a global climate model (GCM) to capture the large-scale dynamics with a 150-km grid cell domain. Within the GCM, they nested a more detailed model (WRF, or weather research and forecast) within the GCM to simulate the storm over California. WRF model output includes 2-km cells of hourly rainfall over a large portion of southern California. Part of the motivation for constructing this storm simulation was to understand the hazards associated with such storms, including shallow landslides.

Most shallow landslide susceptibility models tend to overpredict the number of failures actually triggered by historic storms (e.g., Fig. 1), even where calibrated. A number of recent workers have used intensive site characterizations to calibrate physically-based models of slope stability (e.g., Godt *et alii*, 2008). Where they have been successfully calibrated at field sites, such models represent the optimal method to forecast landslide abundance from simulation storms over small areas. Extending such forecasts across broad regions (states or nations) may currently be beyond our capacity, because of the profound difficulty in capturing spatial variations in influential model parameters (e.g., soil depth, transmisivity, friction angle and cohesion)

An alternate approach would use the historical record of landslide occurrences to create threshold values of rainfall intensity for given durations (e.g., Caine, 1980; Cannon & Ellen, 1985, 1988; Wilson & Wieczorek, 1995; Casadei *et alii*, 2003; Godt e*t alii*, 2006; Guzzetti *et alii*, 2007; 2008). The exact location of these thresholds remains problematic, in part because rainfall analyses do not account for important state and material property differences including initial moisture conditions, the rate at which rain enters the soil, the rate at which it leaks into the underlying bedrock, the soil strength properties, and the cohesion due to vegetation roots. They also do not account for variations in topographic convergence and slope that influence soil stability through the routing of subsurface water and the magnitude of the downslope force. All of these variables influence the stability of hillslopes, and we expect them to vary spatially. As a consequence, there is great uncertainty as to the exact location of the threshold between rains that cause

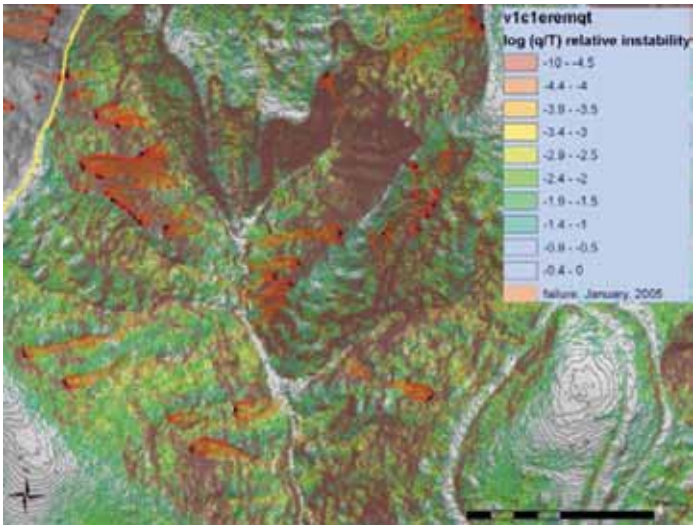

Fig. 1 - January 2005 failures in Ventura on 1-m contour map from LiDAR. Areas of instability represented by green (least unstable), yellow and red (most unstable) colors. Like most models, this shallow slope stability model (Shalstab) vastly over-predicts the areas of instability (~ 1% of unstable areas actually failed)

failures, and those that do not. Recent work (Godt *et alii,* 2008; Chleborad *et alii*, 2008) illustrates that progress on these thresholds will require better data on transient water content and soil properties..

We use elements of both approaches to attempt to forecast landslide abundance for the Arkstorm simulation. Despite uncertainty about the exact rainfall thresholds for landslide generation, most believe that storms with more intense, longer lasting rainfalls will trigger more shallow landslides. We use historic rainfall records and digital maps of consequent shallow failures to estimate a storm rainfall metric that scales with shallow landslide abundance. We refine this scaling by using topographically-based landslide susceptibility models to account for regional variations in stability associated with varying topography (e.g., slope or convergence). We present these findings as a graph of the fraction of model cells predicted to be unstable as a function of rainfall intensity. A regression through this relation allows us to extrapolate it across the storm rainfall domain to forecast shallow landslide abundance.

METHODS

MAPPING

In southern California, USA, rainfall-induced landslides have been triggered by short-duration, high-intensity monsoonal storms (e.g., Morton and Hauser, 2001), spring snowmelt (e.g., Morton & Campbell, 1978), and large winter storms. Winter storms include atmospheric river events and are arguably responsible for the most widespread historic landslide events (e.g., January 1969). Morton mapped shallow landslides and debris flow runouts from winter storms using air photos. Alvarez digitized landslide initiation points and debris flow runouts by transferring air photo interpretations to digital raster graphs of USGS 7.5' quadrangles by hand. In the Santa Paula area, Morton & Alvarez mapped landslides that occurred during storms in 1969, 1998, 2001 and 2005 (Fig 2). These shallow landslides occur in weak Plio-Pleistocene rocks with high clay and silt contents (e.g., Tan et al., 2004). Landslides in these weak rocks tend to be wide (> 3m), shallow (< 2m) failures of colluvium that extend to whole sections of hillslopes. In the Sunland area of Los Angeles, they mapped landslides and debris flows from 1998, and 2005 storms. Rocks in this area are also predominately weak Plio-Pleistocene sediments with high silt and clay fractions.

In the San Francisco Bay area of northern California, USA, Wentworth (1986) used air photographs to map shallow landslides and debris flows triggered by storms in December 1955 and January 1982 in the Montara area. In this detailed area, Wentworth's mapped failures are more accurately located than the

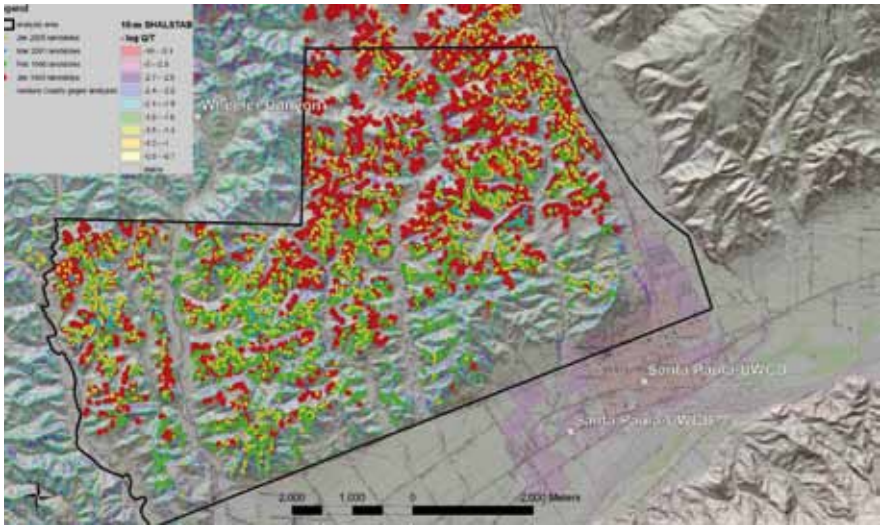

Fig. 2 - Map of Santa Paula analysis area, southern California showing historic landslides mapped by Morton and Alvarez. Failures date from 1969 (red), 1998 (green), 2001 (blue), and 2005 (yellow). Rain gage locations shown by white dots. Relative landslide susceptibility shown by yellow (low) to red(high) colors from Shalstab model with zero cohesion and 45 degrees friction angle

regional maps of landslide initiation points for the entire Bay Area region in Ellen & Wieczorek (1988). Stock used digital imagery from before and after the December 31, 2005 storm to add recent landslide headscarps, lateral scarps and displaced mass (or runout). He used air photos from 1943 and 1973 to estimate the number of shallow landslides within this area (see Table 1). Stock also used 1-m LiDAR and time sequence digital imagery to map shallow and deep-seated landslides in the Ventura region (e.g., Fig. 1).

HISTORIC AND SIMULATED RAINFALL

Just to the south of the Santa Paula analysis area in southern California, the Wheeler rain gage records hourly and daily rain beginning in 1966, although it lacks hourly data for a 2001 storm. The Santa Paula gages record hourly data since 1961, and include all of the storms of interest. We use the Wheeler record to rank the 24- and 48-hour storm history, and the Santa Paula gages for the hourly analysis. In the Sunland area, the closest hourly rain gage at Hanson dam is in a rain shadow from the Verdugo hills to its southeast. The nearest other rain gage with an hourly record is at Pacoima dam, 5 km to the north. This hourly record commences in 1997, and we use it to characterize rainfall intensities during the 1998 and 2005 landslides in Sunland

Prior to the 2002 installation of an hourly station (Spring Valley) near Pilarcitos, northen California, the closest hourly rainfall data for the Montara analysis area was from San Francisco International Airport (SFO). San Francisco Public Utilities Commission (SFPUC) has operated four daily rain gages in the Montara area, of which the Pilarcitos dam gage (1916-present) is the closest. The other three gages are in upper and lower Crystal Springs reservoir, and San Andreas reservoir, along the San Andreas Fault. We use the Pilarcitos record to rank the 24- and 48-hour storm intensity since 1916, and the Spring Valley RAWS station to calculate hourly data for the 2005 storm. We apply the pattern of rainfall at SFO hourly gage to the Pillarcitos daily data to estimate 12-hour rainfall intensity at Pillarcitos during the December 1955 and January 1982 storms. We use the daily totals

calibration area	landslide activity (number in area)	source	date of max. 24-hour rain ending at 08:00 on:	48-hour intensity (mm/hr)	24-hour intensity (mm/hr)	prior day (mm)	prior 7 day or continuous (mm)	antecedant rain from Sept 1 (mm)
Santa Paula, S. CA	**2148**	Morton & Alvarez, unpub.	**1/10/2005**	**7.2**	**8.1**	**153**	**274**	**725**
from 1966,	**6325**	Morton & Alvarez, unpub.	**1/25/1969**	**5.3**	**9.2**	**34**	**344**	**466**
Wheeler #225	?		1/10/1995	5.1	6.6	87	218	324
	?		2/17/1980	4.5	8.0	22	64	360
	?		2/10/1978	4.3	6.1	59	117	512
	?		12/4/1974	4.2	8.3	0	0	21
	<2148	Morton & Alvarez, unpub.	**1/9/2005**	**4.0**	**6.4**	**41**	**121**	**572**
	?		***2/25/1969***	***4.0***	***5.7***	***56***	***85***	***931***
	2448	Morton & Alvarez, unpub.	**2/8/1998**	**3.9**	**4.8**	**73**	**283**	**655**
	<6325	Morton & Alvarez, unpub.	**1/20/1969**	**3.8**	**5.3**	**56**	**89**	**178**
	?		11/29/1970	3.7	7.4	1	10	23
	?		2/11/1973	3.5	6.4	12	101	431
	?		1/5/2008	3.5	7.0	0	0	115
	?		3/4/1978	3.3	6.0	17	120	824
	?		3/11/1995	3.1	5.9	10	81	900
	?		1/11/2001	3.1	6.3	0	6	79
	382	Morton & Alvarez, unpub.	**3/5/2001**	**3.0**	**6.0**	**0**	**71**	**498**
	?		12/6/1997	2.8	5.5	0	25	107
	?		2/26/2004	2.7	5.4	0	76	264
	?		12/28/2004	2.5	4.7	6	6	227
Montara, N. CA	?		10/13/1962	6.2	5.9	156	202	221
from 1916,	**1400**	Wentworth, 1986	**12/23/1955**	**5.3**	**5.7**	**117**	**252**	**524**
Pillarcitos Dam,	**996**	Wentworth, 1986	**1/5/1982**	**4.3**	**6.9**	**42**	**157**	**685**
SFPUC	?		10/12/1962	4.0	6.5	39	46	65
	?		1/21/1967	3.6	6.6	12	12	380
	?		1/2/1916	3.2	6.2	5	16	NA
	>1		**1/12/1998**	**3.1**	**5.4**	**19**	**162**	**611**
	?		1/2/1997	3.1	4.7	39	114	642
	?		11/6/1973	3.1	6.2	0	0	107
	?		11/6/1994	3.0	4.8	29	30	35
	?		2/11/1919	2.9	5.0	22	146	587
	>14	10-11-43 airphotos	**1/21/1943**	**2.9**	**5.0**	**16**	**16**	**528**
	?		12/14/2002	2.8	4.7	21	53	171
	?		1/21/1970	2.7	4.7	16	220	687
	?		1/17/1950	2.7	5.2	6	144	345
	< 1400	Wentworth, 1986	**12/22/1955**	**2.7**	**4.9**	**11**	**136**	**407**
	61	Stock, unpub.	**12/31/2005**	**2.6**	**5.1**	**2**	**281**	**465**
	?		1/13/1931	2.5	5.1	0	30	276
	?		11/17/1942	2.5	5.0	0	25	80
	?		12/6/1969	2.4	4.7	0	1	113

Tab. 1 - Top 20 daily rainfall events in calibration areas

from the surrounding SFPUC gages to evaluate the presence or absence of orographic forcing in the 1955 and 1982 storms..

We used the daily data to calculate the antecedent rainfall from 1st September up to the day of storm (summer rainfall totals are commonly negligible in these areas). Numerous previous studies (e.g., Campbell, 1975; Nilsen *et alii*, 1977; Wilson *et alii*, 1993) reported that 10-15" (254-381 mm) of rainfall were required before storms triggered shallow landslides. Larger antecedent totals are presumed to correspond to higher matric water content (i.e., lower suction values in the soil), reducing the amount of rain and time required to generate pore water pressure in the soil. We used daily totals to calculate the sum of rainfall to the fieldsites from the previous 7 days, or continuous rainfall period (days with non-zero rain). We hypothesize that high 7-day precursor rainfalls are likely to result in very low soil suction, so that additional rainfall infills pores, generating positive pore water pressure. We also calculated the rainfall total preceding the day of peak rainfall intensity. We hypothesized that high prior-day rainfalls in combination with high antecedent rain might lead to rapid generation of positive pore water pressures in many areas

For the Arkstorm simulation storm, Dettinger *et alii* (2011) provided hourly rainfall totals on a 2-km grid in southern California, and a 6-km grid over the whole state. We imported their ASCII data into ArcGIS and created hourly 2.5 km grids of rainfall intensity for storm simulation days 6-8, corresponding to the January 26-28, 1969 period of most intense rainfall. We increased the grid-cell size to 2.5 km to cover gaps in data introduced by gridding their lattice which is oriented at ~ 45 degrees from N-S

We used Shalstab to estimate relative susceptibility to shallow landslides initiated by storm rainfall. Shalstab (Dietrich *et alii*, 1995; 2001; Montgomery & Dietrich, 1994; Bellugi *et alii*, this volume) uses an infinite slope approximation, and assumes steady input of rainfall that infiltrates the soil and flows down-slope in the subsurface, parallel to the gradient (Dupuit-Forcheimer assumption). On a cell-by-cell basis, it calculates the ratio of drainage area to the product of cell width and sine of the slope, an approximation of the ratio of rainfall rate (q) to the depth integrated hydraulic conductivity (T). The q/T ratio controls saturation in the soil column, a measure of relative instability. Shalstab allows estimates of the effect of soil strength (friction and cohesion) on stability, but the spatial variability of these parameters due to soil properties and vegetation has resisted quantification. As a consequence, its use on a regional area usually neglects variations in soil strength and hydraulic properties. It also assumes a steady-state balance between rainfall and subsurface flow, a condition that is exceedingly unlikely during the fluctuating rainfall intensities that accompany most storms. A further limitation of the model is its neglect of lateral forces that likely play a role in convergent areas of the topography..

Despite these very real limitations, Shalstab offers an ability to estimate relative differences in landslide susceptibility due to differences in both slope and topographic convergence. Where landslides are concentrated in hollows, it is particularly successful at predicting the locations of shallow failures. To the extent that landslides occupy planar or divergent topography as resolved by the DEM, Shalstab is less likely to capture instability. 10-m DEM's tend to under-represent both convergence and slope within 1-2 grid cells of the ridgeline. As a consequence, landslides that initiate close to ridge-tops are rarely predicted by 10-m Shalstab runs. In some landscapes, this fraction may approach 25% or so of the total landslide inventory.

We compiled 10-m DEM's from the National Elevation Dataset (NED), and removed sinks using ArcGIS's sink removal algorithm. We ran the default version of Shalstab on 10-m USGS grids of California, assuming zero cohesion and a friction angle of 45 degrees (Bellugi *et alii*, this volume). These default parameters have a tendency to maximize the areas of likely instability, a useful result for comparing susceptibility between landscapes using slope and convergence as topographic metrics. They are not meant to represent site-specific values of cohesion, whose use would reduce the total area of instability.

RESULTS

RAINFALL

Table 1 ranks the top twenty daily rainfall events in Santa Paula and Montara by their 48-hour totals (peak rainfall day plus previous day). These days appear to encompass the major known landslide producing storms at both sites, although the Montara daily totals omit a high intensity storm that caused a few landslides observed in 1973 airphotos. Within these

top twenty rainfall events (all above 4 mm/hour 24-hour intensity), landslide occurrences in both Santa Paula and Montara have antecedent rainfalls exceeding 400 mm. This value is consistent with those from previous studies (Campbell, 1975; Nilsen *et alii*, 1977) on large winter storms. Above this antecedent rainfall, neither area has a consistent relation between 24-hour intensity and landslide abundance. Landslide abundance at Montara does scale with 48-hour intensity, although this relation does not hold for Santa Paula because of the short duration, high-intensity 1998 storm. Landslide abundance at Santa Paula scales with the 7-day prior rainfall totals, but again this relation does not hold at Montara. Daily or multi-day rainfall cannot be used alone as a proxy for landslide abundance at these sites.

Table 2 lists the hourly rainfall intensities for the peak rainfall intensity day associated with each of our landslide inventory storms. Values for some of the antecedent rainfalls are somewhat different from Table 1 where hourly data are available at Santa Paula. Peak hourly intensities on these days range from 10-34 mm/hour. There is no clear relation between these short duration intensities and landslide abundance. For instance, a peak hourly intensity of 25 mm/hr in 1998 produces fewer landslides at Santa Paula than the lower maximum hourly intensity of 20 mm/hr from the 1969 storm. Figure 3 summarizes intensity and duration for landslide-producing storms at Santa Paula. The figure illustrates that although the 1998 storm was intense at short time scales, the 1969 storm has higher intensities at all periods greater than 1-2 hours. At 3-8 hour rainfall durations, relative landslide abundance in Table 1 scales with storm intensity at Santa Paula. The scaling most closely mimics landslide abundance at 6-hour durations, where similar landslide abundances

mimic similar values for 1998 and 2005 storm intensities. For this reason, we choose the 6-hour intensities from Santa Paula as a storm metric that scales with landslide abundance in this region.

Analysis of SFO and Spring Valley gages near Montara indicated that intensities at SFO are systematically lower than at the higher elevation Spring Valley gage, closest to the landslide analysis area. These comparisons, in addition to those showing the strong orographic effect on daily rainfall between Pilarcitos and lower elevation gages for the 1955 event, indicate that the 6-hour intensity pattern detected in the Santa Paula data cannot be reconstructed for the Montara area. For this reason, we restrict our simulations to the southern California sites.

We used the hourly rainfall data from the Ark-

calibration area	day of max 6-hour intensity	antecedant rain from Sept 1 (mm)	prior 7 day or continuous (mm)	prior day (mm)	1-hour intensity (mm/hr)	3-hour intensity (mm/hr)	6-hour intensity (mm/hr)	12-hour intensity (mm/hr)	12-hour integral (mm)	24-hour intensity (mm/hr)	48-hour intensity (mm/hr)	fraction of unstable model cells failed
Santa Paula, S. CA	1/25/1969	466	274	153	20.3	19.4	18.6	15.8	215	9.7	5.7	0.0258
from 1961 at	2/7/1998	655	283	73	25.9	18.5	12.8	6.6	141	3.4	2.9	0.0099
Santa Paula #245, #245A	1/9/2005	572	121	41	14.7	11.5	10.4	9.4	125	6.0	3.8	0.0085
	3/5/2001	498	71	0	10.9	7.1	6.6	5.6	80	4.8	2.8	0.0015
Sunland, S. CA	2/7/1998	689	99	103	34.2	18.7	11.9	6.0	143	3.0	2.2	0.0066
from 1997 at	1/9/2005	524	75	48	19.0	8.7	8.5	6.8	103	5.5	4.3	0.0042
Pacoima dam gage #33												
Montara, N. CA	12/31/2005	465	281	2	16.2	13.0	10.3	9.0/***9.6***	126	5.2	2.6	0.0001
from 2002 at	1/5/1982	685	157	42	NA	NA	NA	***11.0***	NA	6.8	4.3	0.0014
Spring Valley # HSPC1	12/23/1955	524	252	117	NA	NA	NA	***9.0***	NA	5.7	5.3	0.0020

Tab. 2 - Hourly rainfall and SHALSTAB results in calibration areas

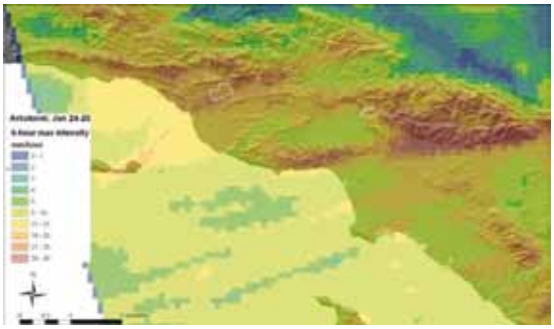

Fig. 4 - Map of maximum 6-hour rainfall intensity for the Jan 24-26 Arkstorm simulation. Santa Paula and Sunland analyses areas shown by white polygons. 2.5 km grid cells are generated by averaging hourly rainfalls over a 6-hour moving window, and then extracting the maximum value at any point on the grid

storm simulation (Dettinger *et alii*, 2011) to calculate the grid of maximum 6-hour rainfall intensities across the Southern California landscape (Fig. 4). This figure mirrors the peak hourly intensity grid in that the highest rainfall intensities are distributed at mountain fronts (e.g., Santa Ynez, Santa Monica, San Gabriels) where orographic effects intensify rainfall rates. Note the rainfall intensity low just to the south of the Sunland analysis area, which is where the Hanson dam rain gage is located.

SHALSTAB LANDSLIDE MODEL

Figure 5 illustrates a subset of the the pattern of shallow landslide susceptibility for southern California. At this small scale the visible pattern is dominated by red and purple areas that correspond to steep, often cliff-forming topography in the Santa Ynez and San Gabriel ranges. To the extent that these areas are dominated by rock outcrop and patchy colluvium, they may actually be less likely to fail as shallow landslides

A MODEL FOR FORECASTING CRUDE LANDSLIDE FREQUENCY GIVEN RAINFALL SIMULATIONS

Figure 6 plots the fraction of unstable Shalstab cells that actually failed versus the maximum 6-hour intensity. At the Santa Paula site, as 6-hour storm intensity increased from ~ 5 mm/hr (2001) to 16 mm/hr (1969), the number of failures increased and the fraction of the unstable areas predicted by Shalstab that actually failed increased from 0.0015 to 0.025 as the power law:

$$f = .00001\, I_{6\text{-}hr}^{2.7}$$

The 2005 data from Montara illustrate that, at the very least, the intercept from (1) may not apply to northern California sites. Consequently, we limit our analyses to the southern California rainfall simulation area. We apply (1) to each of the 2.5 km^2 cells representing maximum 6-hour rainfall intensity for the Arkstorm. We derive a matching grid whose values represent the number of unstable 10-m cells within each 2.5 km^2 cell. We multiply these grids together to obtain a grid showing the number of shallow landslides for the simulation storm.

The pattern of landslide numbers in Figure 7 mimics the pattern of 6-hour maximum rainfall intensity of Figure 3. Santa Ynez, Santa Monica and San Gabriel ranges are characterized by landslide densities of 1-3,000 per cell. The analysis areas of Santa Paula and Sunland have densities of 200-1000 landslide per cell, reflecting their role in generating (1). Lowland areas have densities of 10 or less, largely concentrated at cut banks on rivers or terraces.

DISCUSSION AND CONCLUDING REMARKS

How generalizable is Figure 7? The weak rocks characterizing the Santa Paula calibration area, and Sunland, have soils that fail at densities that tend to exceed those observed in soils developed on older, stronger lithologies. Widespread areas of very thin soils and bedrock in the steepest parts of the Santa Ynez and San Gabriel Mountains are also not likely to fail as

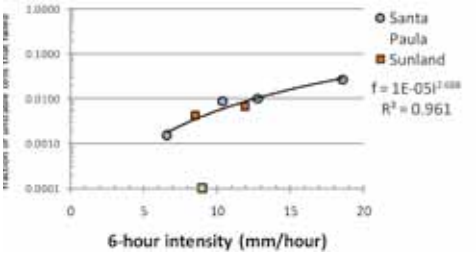

Fig. 6 - Plot of 6-hour rainfall intensity vs. fraction of unstable model cells that failed. Regression from Santa Paula data

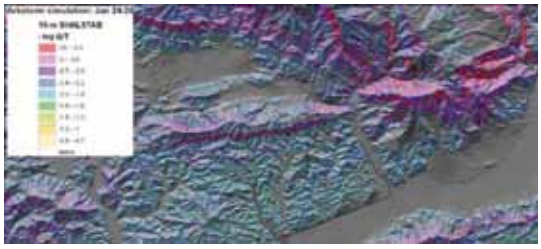

Fig. 5 - Map of Ventura and Santa Paula area illustrating Shalstab output for 45 degrees friction angle and zero cohesion on the 10-m DEM. Relative landslide susceptibility shown by yellow (low) to red (high) colors. Note broad areas of red that correspond to cliff-forming units in Tertiary sedimentary units. Some of these areas are likely characterized by rockfall processes, not shallow landslides

shallow landslides during large rainfall events. Figure 7 shows the regions of weak Quaternary, Pliocene and Miocene rocks in southern California that can be expected to have similar, if not exactly the same attributes as the calibration area. These hachured areas encompass many of the residential areas of southern California. High landslide numbers forecast within these areas are a reflection of the abundance of failures observed during the winter storms of 1969.

Figure 7 and equation 1 are crude, preliminary efforts at forecasting the regional effects of large storms on shallow landslide abundance by combing rainfall metrics with a shallow landslide susceptibility model. They do not account for deep-seated landfslides, or steep areas of bedrock or patchy soil where rockfall predominates. As is evident from the lack of hourly data at Montara, testing the generality of the form of (1) will require accurately mapping the distribution and style of failures in the vicinity of hourly rain gages. It is clear from recent work (e.g., Baum et al., 2005; Godt *et alii*, 2008; Chleborad *et alii*, 2008) that understanding which rainfall intensities generate positive pore water pressures increasing the probability of failure will require monitoring efforts in some of the historic mapping areas. In combination with geotechnical and hydraulic properties of soils, these kinds of monitoring data will provide an expectation for the rainfall intensities and durations that generate large numbers of landslides. Two such sites are currently active in the Bay Area as part of the U.S. Geological Survey Bay Area Landslide Task (BALT). They are providing data on soil moisture, pore water pressure and local hourly rainfall that will help us calibrate the next generation of forecasting models for landslide thresholds and abundance.

ACKNOWLEDGEMENTS

We thank David Strong for compiling and merging the 10-m data. Maiana Hanshaw and Nichole Kneupprath compiled much of the rain gage data. Bruce McGurk of SFPUC provided the wonderfully long daily rainfall records of Pillarcitos and other SFPUC gages in the Montara area. Mike Dettinger provided ASCII files and Fortran code to extract the storm simulation data. Geoff Phelps and Bruce Chuchel modified this code to extract hourly values. This research used resources of the National Energy Research Scientific Computing Center, which is supported by the Office of Science of the U.S. Department of Energy under Contract No. DE-AC02-05CH11231. Further technical support was offered by the Berkeley UPC group. We thank Brian Collins, Douglas Morton, Mark Reid, and Carl Wentworth who provided insightful reviews.

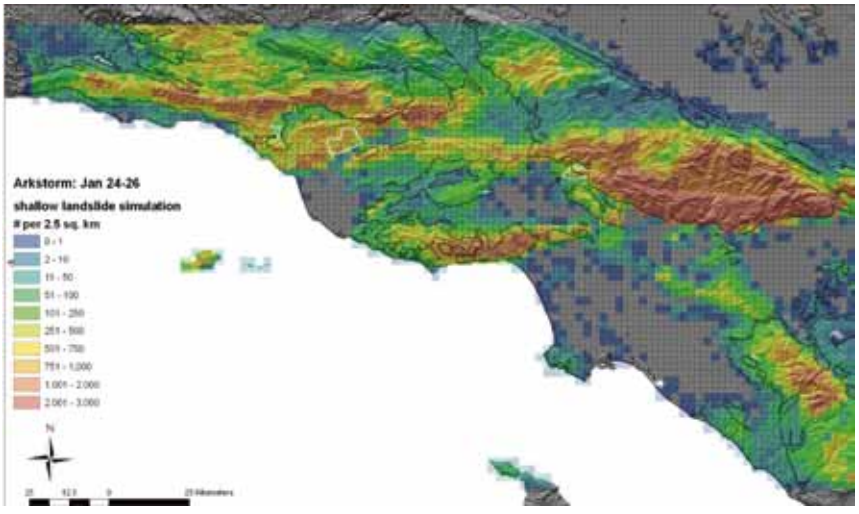

Fig. 7 - Quaternary, Pliocene and Miocene sedimentary rocks (hachured area) superimposed on the forecast for landslide abundance resulting from the Arkstorm. Cells within the hachured area have rock types similar to the calibration area at Santa Paula. Cells outside these zones likely overestimate the number of landslides because 1) rock units produce stronger soils and 2) different processes (e.g. rockfall) dominate erosion. Gray areas have no unstable cells in 10-m data. Calibration (Santa Paula) and test (Sunland) areas shown by white polygons

REFERENCES

Baum R.L., Godt J.W., Harp E.L., McKenna J.P. & McMullen,S.R. (2005) - *Early Warning of Landslides for Rail Traffic Between Seattle and Everett, Washington, USA.* In Hungr O., Fell R., Couture R. & Bernhard E., eds., *Landslide Risk Management*, Proceedings of the 2005 International Conference on Landslide Risk Management: New York, A.A. Balkema, p. 731-740.

Bellugi D., Dietrich WE., Stock J., McKean J., Kazian B. & Hargrove P. (this volume) - *Spatially explicit shallow landslide susceptibility mapping over large areas.* Proceedings of the 5th International Conference on Debris-Flow Hazards Mitigation: Mechanics, Prediction and Assessment, Italian Journal of Engineering Geology and Environment.

Caine N. (1980) - *The rainfall intensity-duration control of shallow landslides and debris flows.* Geogr. Ann. **62A**: 23–27.

Campbell R.H. (1975) - *Soil slips, debris flows, and rainstorms in the Santa Monica Mountains and vicinity, southern California.* U.S. Geological Survey Prof. Paper 851, 51 pp.

Cannon S.H. & Ellen S.D. (1985) - *Rainfall conditions for abundant debris avalanches.* San Francisco Bay Region, California. Calif. Geol., **38**: 12267–12272.

Cannon S.H. & Ellen S.D. (1988) - *Rainfall that resulted in abundant debris-flow activity during the storm.* In: Ellen S.D. & Wieczorek G.F. (eds) *Landslides, floods and marine effects of the storm of January 3–5, 1982 in the San Francisco Bay Region, California.* U.S. Geological Survey Prof. Paper 1434:27–34.

Cannon S.H. (2005) - *A NOAA–USGS demonstration flash-flood and debris-flow early-warning system.* U.S. Geological Survey Fact Sheet 2005-3104. Prepared in cooperation with National Oceanic and Atmospheric Administration (NOAA).

Casadei M., Dietrich W.E. & Miller N.L. (2003) - *Testing a model for predicting the timing and location of shallow landslide initiation in soil mantled landscapes.* Earth Surface Processes and Landforms, **28**: 925-950.

Chleborad A.F., Baum R.L., & Godt J.W. *(2008) - A prototype system for forecasting landslides in the Seattle, Washington, Area,* In: Baum R.L., Godt J.W. & Highland L.M., eds., *Engineering geology and landslides of the Seattle, Washington area*. Geological Society of America Reviews in Engineering Geology, XX; 103-120, doi: 10.1130/2008.4020(06).

Coe J.A. & Godt J.W. (2001) - *Debris flows triggered by the El Nino rainstorm of February 23, 1998, Walpert Ridge and vicinity, Alameda County, California. Reston, Virginia.* U.S. Geological Survey Miscellaneous Field Studies Map MF-2384.

Dettinger M., Ralph F.M., M. Hughes M., Das T., Neiman P., Cox D., Estes G., Reynolds D., Hartman R., Cayan D. & Jones L. (2011) - *Requirements and designs for a winter storm scenario for emergency preparedness and planning exercises in California.* Weather, Climate and Society.

Dietrich W.E., Reiss R., Hsu M. & Montgomery D.R. (1995) - *A process-based model for colluvial soil depth and shallow landsliding using digital elevation data.* Hydrological Processes, **9**: 383-400.

Dietrich W.E., Bellugi D., & Real de Asua R. (2001) - *Validation of the shallow landslide model, Shalstab, for forest management.* In Wigmosta M.S. & Burges S.J. (eds), *Land Use and Watersheds: Human influence on hydrology and geomorphology in urban and forest areas*. Amer. Geoph. Union, Water Science and Application, **2**: 195-227.

Ellen S.D. & Wieczorek G.F. (1988) - *Landslides, floods, and marine effects of the storm of January 3–5, 1982, in the San Francisco Bay region, California.* U.S. Geological Surve. Prof. Paper 1434.

Godt, J.W., Baum., R.L., & Chleborad, A.F. *(2006) - Rainfall characteristics for shallow landsliding in Seattle, Washington, USA, Earth Surface Processes and Landforms, 31:97–110.*

Godt J.W., Schulz W.H., Baum R.L. & Savage W.Z. *(2008) - Modeling rainfall conditions for shallow landsliding in Seattle, Washington.* In: Baum R.L., Godt J.W. & Highland L.M., eds., *Landslides and Engineering Geology of the Seattle, Washington area.* Geological Society of America Reviews in Engineering Geology, **XX**: 137-152, DOI: 10.1130/2008.4020(08).

Godt J.W. (editor), Arnal C.H., Baum R.L., Brien D.L., Coe J.A., De Mouthe J., Ellis W.L., Graymer R.W., Harp E.L., Hillhouse J.W., Houdre N., Howell D.G., Jayko A.S., Lajoie K.R., Morrissey M.M., Ramsey D.W., Savage W.Z., Schuster R.L., Wieczorek G.F. & Wilson R.C. (1999) - *Maps showing locations of damaging landslides caused by El Nino rainstorms, winter season 1997_98, San Francisco Bay region, California.* Reston, Virginia: U.S. Geological Survey Miscellaneous Field Studies Maps MF-2325- A-J. Available from: http://pubs.usgs.gov/mf/1999/mf-2325/, accessed on 25 November, 2008.

Guzzetti F., Peruccacci S., Rossi M. & Stark C.P. (2007) - *Rainfall thresholds for the initiation of landslides in central and southern Europe.* Meteorology and Atmospheric Physics, **98**: 239-267.

Guzzetti F., Peruccacci S., Rossi M. & Stark C.P. (2008) - *The rainfall intensity-duration control of shallow landslides and debris flows: an update.* Landslides, **5**: 3-17.

Montgomery D. R. & Dietrich W.E. (1994) - *A physically-based model for topographic control on shallow landsliding.* Water Resources Research, **30**(4): 1153-1171.

Montgomery D.R., Schmidt K.M., Dietrich W.E. & McKean J. (2009) - *Instrumental record of debris flow initiation during natural rainfall: Implications for modeling slope stability.* J. Geophy. Research- Earth Surface, **114**: F01031, doi:10.1029/2008JF001078, 15 pp.

Morton D.M. & Hauser R.M. (2001) - *A debris avalanche at Forest Falls, San Bernardino County, California, July 11, 1999:* U.S. Geological Survey Open-File Report 01-146. CD ROM and web; http://geopubs.wr.usgs.gov/open-file/of01-146.

Morton D.M. & Campbell R.H. *(1978) - Cyclic landsliding at Wrightwood, southern California - A preliminary report.* U.S. Geological survey Open File Report 78-1079.

Nilsen T.H., Taylor F.A. & Dean R.M. (1976a) - *Natural conditions that control landsliding in the San Francisco Bay region - An analysis based on data from the 1968-69 and 1972-73 rainy seasons.* U.S. Geological Survey Bull. 1424, 35 pp.

Nilsen T.H &Turner B.L. (1975) - *Influence of rainfall and ancient landslide deposits on recent landslides (1950–71) in urban areas of Contra Costa Country, California.* U.S. Geological Survey Bull. 1388.

Nilsen T.H., Taylor F.A.& Brabb E.E. (1976) - *Recent landslides in Alameda County, California (1940–71) an estimate of economic losses and correlations with slope, rainfall, and ancient landslide deposits.* U.S. Geological Survey Bull. 1398.

Rice R.M. & Foggin G.T. (1971) - *Effects of high-intensity storms on soil slippage on mountainous watersheds in Southern California.* Water Resour Res, **7**: 1485-1496.

Schimmelmann A., Lange C.B.& Meggers B.L. (2003) - *Palaeoclimatic and archaeological evidence for a ~200-yr recurrence of floods and droughts linking California, Mesoamerica and South America over the past 2000 years.* The Holocene, **13**: 763-778.

Tan S.S., Clahan K.B. & Irvine P.J. (2004) - *Geologic map of the Santa Paula 7.5-minute quadrangle, Ventura County, California.* A digital database: California Geological Survey, Preliminary Geologic Maps, scale 1:24,000.

Taylor F.A. & Brabb E.E. (1972) - *Maps showing distribution and cost by counties of structurally damaging landslides in the San Francisco Bay region, California, winter of 1968-69.* Reston, Virginia: U.S. Geological Survey Miscellaneous Field Studies Map MF-327.

Taylor F.A., Nilsen T.H. & Dean R.M. (1975) - *Distribution and cost of landslides that have damaged manmade structures during the rainy season of 1972-1973 in the San Francisco Bay region, California.* Reston, Virginia: U.S. Geological Survey Miscellaneous Field Studies Map MF-679.

Wilson R.C. & Wieczorek G.F. *(1995) - Rainfall thresholds for initiation of debris flows at La Honda, California.* Environ Eng Geosci., **1**: 11–27.

Wilson R.C., Mark R.K. & Barbato G. (1993) - *Operation of a realtime warning system for debris flows in the San Francisco Bay area, California.* In: Shen H.W., Su S.T. & Wen F. (eds) Hydraulic Engineering '93. Proc 1993 Environmental Geology 35 (2–3) August 1998 7 Q Springer-Verlag.

Wentworth C.M. (1986) - *Maps of debris flow features evident after the storms of December 1955 and January 1982, Montara Mountain area, California.* U.S. Geological Survey Open-File Map 86-363, 2 sheets at 1:24,000 scale